TOXICOLOGICAL SCIENCES **119(1)**, 104–115 (2011)
doi:10.1093/toxsci/kfq330
Advance Access publication October 27, 2010

Effects of the Protein Kinase Inhibitor PKC412 on Gene Expression and Link to Physiological Effects in Zebrafish *Danio rerio* Eleuthero-Embryos

Daniela M. Oggier,*,† Anna Lenard,‡ Michael Küry,* Birgit Hoeger,§ Markus Affolter,‡ and Karl Fent*,¶,[1]

*University of Applied Sciences Northwestern Switzerland, School of Life Sciences, CH-4132 Muttenz, Switzerland; †Division of Limnology, University of Zürich, Institute of Plant Biology, CH-8802 Kilchberg, Switzerland; ‡Biozentrum der Universität Basel, CH-4056 Basel, Switzerland; §Novartis Pharma AG, Schwarzwaldallee 215, CH-4058 Basel, Switzerland; and ¶Department of Environmental Sciences, Swiss Federal Institute of Technology (ETHZ), CH-8092 Zürich, Switzerland

[1]To whom correspondence should be addressed at University of Applied Sciences Northwestern Switzerland, School of Life Sciences, Gründenstrasse 40, CH-4132 Muttenz, Switzerland. Fax: +0041-61-467-44-60. E-mail: karl.fent@fhnw.ch or karl.fent@bluewin.ch.

Received August 14, 2010; accepted October 4, 2010

To identify molecular effects of the antineoplastic agent protein kinase C inhibitor 412 (PKC412) (midostaurin), we applied gene expression profiling in zebrafish using whole-genome microarrays. Behavioral, developmental, and physiological effects were investigated in order to analyze for correlations between altered gene expression profiles with effects on development and physiology. Zebrafish blastula-stage embryos were exposed for 6 days postfertilization to nominal levels of 2 and 40 μg/l PKC412. Among the 259 and 511 altered transcripts at both concentrations, respectively, the expressions of genes involved in the circadian rhythm were further investigated. Alteration of swimming behavior was not observed. Pathways of interest affected by PKC412 were angiogenesis, apoptosis, DNA damage response, and response to oxidative stress. Angiogenesis was analyzed in double-transgenic zebrafish embryos Tg(fli1a:EGFP)y1;Tg(gata1:dsRed)sd2; no major defects were induced by PKC412 treatment at both concentrations. Apoptosis occurred in olfactory placodes of embryos exposed to 40 μg/l, and DNA damage was induced at both PKC412 concentrations. However, there were no significant effects on reactive oxygen species formation. This study leads to the conclusion that PKC412-induced alterations of gene transcripts are partly paralleled by physiological effects at high, but not at low PKC412 concentrations expected to be of environmental relevance.

Key Words: **PKC412; *Danio rerio*; transgenic zebrafish; microarray; angiogenesis; apoptosis.**

Antineoplastic agents have widespread use in cancer treatment. They include different classes, such as antibodies, protein kinase inhibitors (such as protein kinase C inhibitor 412 [PKC412]), topoisomerase I and II inhibitors, antimetabolites, alkylating agents, and others (Chabner *et al.*, 2006). Antineoplastic agents are mainly found in the nanograms per liter to the lower micrograms per liter range in effluents (Fent *et al.*, 2006; Monteiro and Boxall, 2010). For example, ifosfamide was found in Germany up to a concentration of 2.9 μg/l (Ternes, 1998).

As many pharmacological targets are evolutionary conserved, antineoplastic agents are supposed to have similar effects in aquatic organisms as in humans (Christen *et al.*, 2010; Gunnarsson *et al.*, 2008; Jones *et al.*, 2007) Therefore, environmental exposure may pose a risk for negative effects on nontarget species because of the mutagenic and cancerogenic properties of such compounds.

A newly developed antineoplastic agent is midostaurin (PKC412, $\log K_{OW}$ = 4.26; Novartis Pharma AG, Basel, Switzerland; internal data), which belongs to the family of indolocarbazoles and is a selective inhibitor of several isoforms of protein kinase C in humans (Karaman *et al.*, 2008). It is a sugar ring variant of staurosporine, which was originally isolated from *Streptomyces staurosporeus* (Takahashi *et al.*, 1989). PKC412 inhibits a large variety of tyrosine kinases including FMS-like tyrosine kinase (FLT3), platelet-derived growth factor (PDGF) receptors, and c-kit (stem cell factor) receptor (Fabbro *et al.*, 2000). PKC412 has been developed as a therapeutic agent against acute myeloid leukemia because of its ability to inhibit growth, angiogenesis, and P-glycoprotein–mediated multidrug resistance in tumor cells (Fabbro *et al.*, 2000). In addition, PKC412 affects other cellular processes such as immune responses or neuronal functions, as shown by effective inhibition of human T-cell activation, proliferation, and tumor necrosis factor alpha production (Si *et al.*, 2005).

Only very few data are available on the toxicity of PKC412 to organisms that may be exposed via wastewater. Exposure of zebrafish blastula-stage embryos to 100nM (57 μg/l) PKC412 resulted in a curved body axis (Chan *et al.*, 2002). Recent data indicate that the no observed effect concentration (NOEC) of PKC412 was 14 μg/l in a *Danio rerio* early life–stage test and the lowest observed effect concentration for mortality was 43 μg/l. The 96-h LC_{50} in adult *D. rerio* was 25 μg/l and the NOEC 19 μg/l (Novartis Pharma AG, internal data). The estimated predicted environmental concentration is 1.5 μg/l (Novartis Pharma AG, internal data).

Currently, there is a lack of chronic toxicity studies with focus on the modes of action on this pharmaceutical in vertebrates and invertebrates. Furthermore, ecological risk assessments of PKC412 within the framework of the European Medicines Agency (2006), in particular at environmentally realistic concentrations in aquatic organisms, are not publicly available. Ecotoxicological tests used for risk assessments are often not sensitive enough to identify subtle adverse effects of pharmaceuticals. They may be more accurately determined by focusing on the modes of action (Christen *et al.*, 2010; Fent *et al.*, 2006; Runnalls *et al.*, 2007). Therefore, potential environmental consequences of PKC412 are unknown. In detail, data on the gene expression profile and their correlation to environmentally relevant endpoints such as behavior and mortality are missing.

In our present study, we aim at determining the modes of action of this novel antineoplastic agent in zebrafish embryos to clarify its potential molecular effects by analyzing the global gene expression pattern. The toxicogenomics approach allows to identify several thousands of genes and the corresponding expression profiles upon exposure, which will assist in the elucidation of the molecular effects and the compound's modes of action (Robbens *et al.*, 2007). We analyze effects at low concentrations in zebrafish embryos and compare the effects on the transcriptional level with effects on mortality and physiological outcomes. We hypothesize that the response of zebrafish to PKC412 exposure is similar to the human response, as their targets, the protein kinases, are evolutionary conserved. Therefore, we searched for alterations in gene expression patterns associated with cellular signaling (e.g., angiogenesis and apoptosis) and oxidative stress. We also hypothesized that alterations in gene expression—because of multiple endpoints and mechanistic information—are more sensitive than physiological or morphological parameters (although they are perhaps less ecologically relevant) but that the observed molecular effects correlate with and propagate to higher levels of the biological organization. In addition, gene expression analysis may also reveal unknown regulatory mechanisms in fish not directly related to the modes of action of PKC412 in humans.

MATERIALS AND METHODS

Chemicals

PKC412 ($\geq$ 99%, molecular weight: 570.6, $\log K_{OW} = 4.26$) was kindly provided by Novartis Pharma AG. Acetonitrile was purchased from Brunschwig (Basel, Switzerland) and methanol was from Stehelin (Basel, Switzerland). Ammonium formiate, dimethyl sulfoxide (DMSO), formic acid, 4-(2-hydroxyethyl)-1-piperazineethanesulfonic acid (HEPES), $MgCl_2$, NaCl, sucrose, Triton X-100, H_2O_2, 4′,6-diamidino-2-phenylindole (DAPI), and dichlorofluorescein-diacetate (DCFH-DA) were obtained from Sigma-Aldrich (Buchs, Switzerland). 4-2-Aminoethyl-benzensulfonyl fluoride hydrochloride (AEBSF), EDTA, low melting agarose, and Tris-HCl were purchased from AppliChem.GmbH (Darmstadt, Germany). Roti-Histofix (10%) was purchased from Carl Roth GmbH & Co. KG (Karlsruhe, Germany). PBS was obtained from F. Hoffmann-La Roche Ltd (Basel, Switzerland).

Exposure Experiment

For the microarray, behavioral, and toxicity studies, freshly fertilized zebrafish embryos were obtained from Harlan Laboratories Ltd (Itingen, Switzerland). Embryos were transferred to the laboratory and examined under a stereomicroscope. All embryos used in the experiments were at blastula stage (Kimmel *et al.*, 1995). They were placed in 750-ml covered glass beakers of reconstituted water (total hardness of 125 mg/l as $CaCO_3$ and a conductivity of 270 µS/cm) and the appropriate concentration of PKC412 or DMSO (0.01%, solvent control). The water temperature was held constant at 27°C ± 1°C with the photoperiod set at 16:8 h light/dark.

The semistatic exposure setup consisted of six replicates of water control, solvent control (0.01% DMSO), and two PKC412 doses. A total of 100 fertilized eggs per replicate ($n = 6$) were exposed up to 6 days postfertilization (dpf) to nominal concentrations of 2 and 40 µg/l PKC412, respectively. This exposure duration seemed to be appropriate as lethal effects occurred already after 3 dpf in the early life stages test. Every 24 h, lethal and sublethal effects were evaluated, dead embryos or eleuthero-embryos were removed, and the water was changed. The quality of the exposure water was continuously monitored by oxygen concentration determination (> 70%), the pH value (6.7–7.2), and the temperature (27°C ± 1°C). At the end of exposure, eleuthero-embryos were anesthetized in a clove oil solution (Fluka AG, Buchs, Switzerland). A total of 80 eleuthero-embryos per replicate were pooled in RNAlater for microarray and quantitative real time polymerase chain reaction (qRT-PCR). Total RNA was extracted using the RNeasy Mini Kit (Qiagen, Basel, Switzerland).

Chemical Analysis

To determine actual exposure concentrations, 10-ml aliquots of exposure water were taken during the experiment for PKC412 analysis. Water samples of each treatment group were taken at the beginning (0 h) and prior to full water renewal (24 h). This was done three times on different days from different randomly selected replicate tanks. Acetonitrile (2 ml) was added to the water samples for liquid chromatography-mass spectrometry (LC-MS) analysis preparation and then stored at −20°C until analysis. The chemical analysis was performed separately for the microarray experiment, the behavioral experiment, and additional experiments (terminal deoxynucleotidyl transferase dUTP nick end labeling [TUNEL] assay, comet assay and reactive oxygen species [ROS] assay).

PKC412 concentrations were determined by LC-MS. The chromatographic separation was achieved by using an Inertsil ODS-3 column (2.1 × 50 mm; 3 µm particle size) from Ercatech AG (Bern, Switzerland) at a column temperature of 30°C. For the analysis, a binary gradient mixture containing eluent A (0.1% [vol/vol] in formic acid in water:acetonitrile [95:5]) and eluent B (0.1% [vol/vol] in formic acid in water:acetonitrile [5:95]) was used at a flow rate of 0.4 ml/min. The gradient started with a mixture of 60% eluent A and 40% eluent B and increased to 100% eluent B after 4 min. The conditions were held for 1 min, and then the system was set back to the initial conditions. The column was reequilibrated for 2 min before the next injection. Five microliters of the samples were injected. The retention time for PKC412 was 3.3 min. Data were then quantified using DataAnalysis for 6300 Series Ion Trap LC/MC version 3.4. Quantification of PKC412 was based on an external calibration curve.

RNA Isolation, Array Hybridization, and Sample Selection

Total RNA was extracted from zebrafish eleuthero-embryos using the RNeasy Mini Kit (Qiagen). Total RNA concentrations were measured spectrophotometrically using a NanoDrop ND-1000 UV-VIS Spectrophotometer at 260 nm. The integrity of each RNA sample was verified using an Agilent 2100 Bioanalyzer (Agilent Technologies, Basel, Switzerland). Only samples containing a 260/280 nm ratio between 1.8 and 2.1, a 28S/18S ratio between 1.5 and 2, and an RNA integrity number > 8 were processed further. A total of 16 arrays (Agilent 4 × 44 K Zebrafish Microarray) were used, including four for the water control group, four for the solvent control group, four for the 2 µg/l, and four for the 40-µg/l PKC412 dose group. Total RNA samples (600 ng) were reverse transcribed into double-strand complementary DNA

TABLE 1
Primer Sequences for Quantitative Real-Time PCR Analysis

Probe ID	Gene	Sequence accession #	Direction	Sequence	Amplicon size (bp)
—	*RpL13α*		fw	agc tca aga tgg caa cac	100
			rv	ag aag ttc ttc tcg tcc tcc	
A_15_P104624	*abcc4*	NM_001007038	fw	ctg gaa aca cga ctc agc aa	122
			rv	gct cac cag agc att gaa ca	
A_15_P103946	*cry5*	NM_131788.1	fw	cat gga gag aac gaa ctg gg	115
			rv	gtg cag aca agc agc cga ac	
A_15_P196411	*ndrg1l*	NM_200692.1	fw	agc gtc ttt gag ctg gac at	113
			rv	tgg aag gtc agg atg gta gg	
A_15_P544897	*opn1mw2*	NM_182891.2	fw	cca tgg cag ttt aag gca ct	100
			rv	ttt tgt gct gag ctg tga cc	
A_15_P112731	*pdpk1*	NM_001077344.1	fw	cgt tta gag ctg gga acg ag	103
			rv	cgc tgg acc aga tct tta gc	
A_15_P236266	*per1*	NM_001030183.1	fw	atg cgt gca aga agt ggt g	131
			rv	acg tcc tca ttt agc gga ctc	
A_15_P197856	*sos*	XM_685079.2	fw	ctg ccc tca ctt ctc acc tc	109
			rv	cac tgg tcc aca cca aac ac	
A_15_P134231	*xpc*	NM_001045210.1	fw	aag aag tcg gca gtg agg aa	101
			rv	gca tat ttt cac ggc tcc at	

(cDNA) in the presence of RNA poly-A controls with the Agilent One-Color RNA Spike-In Kit. Cyanine 3 (Cy3) labeling and hybridization were performed according to the manufacturer's manual.

After reverse transcription of RNA into double-stranded cDNA, double-strand cDNA was *in vitro* transcribed into complementary RNA (cRNA) in the presence of Cy3-labeled nucleotides using a Low RNA Input Linear Amp Kit +Cy dye (Agilent Technologies), performed at the Functional Genomic Center (ETHZ and University of Zürich, Switzerland). The Cy3-labeled cRNA was purified using an RNeasy Mini Kit (Qiagen), and quality and quantity was determined using a NanoDrop ND-1000 UV-VIS Spectrophotometer and an Agilent 2100 Bioanalyzer, respectively. Only cRNA samples with a total cRNA yield higher than 2 µg and a dye incorporation rate between 9 and 20 pmol/µg were used for hybridization. Cy3-labeled cRNA samples (1.65 µg) were mixed with Agilent blocking solution, subsequently fragmented randomly to 100–200 bp at 65°C with fragmentation buffer, and resuspended in hybridization buffer as provided by the Gene Expression Hybridization Kit (Agilent Technologies). Target cRNA samples (100 µl) were hybridized to the Agilent Zebrafish 4 × 44 K Gene Expression Microarray for 17 h at 65°C. The hybridized arrays were then washed using Agilent GE wash buffers 1 and 2 according to the manufacturer's instructions and scanned by an Agilent Microarray Scanner (Agilent p/n G2565BA) at 5-µm resolution with the green photomultiplier tube set to 100% and a scan area of 61 × 21.6 mm. Image generation and feature extraction were performed using the Agilent Feature Extraction (FE) software version 9.5.3. Quality control was additionally considered before performing the statistical analysis. These included array hybridization pattern inspection: absence of scratches, bubbles, areas of nonhybridization, proper grid alignment, spike performance in controls with a linear dynamic range of five orders of magnitude, and the number of green-feature nonuniformity outliers, which should be below 100 for all samples.

qRT-PCR Analysis

One microgram of total RNA of the microarray experiment template was reverse transcribed using Moloney murine leukemia virus reverse transcriptase (Promega Biosciences Inc., Wallisellen, Switzerland) in the presence of random hexamers (Roche Diagnostics) and deoxynucleoside triphosphate (Sigma-Aldrich). The reaction mixture was incubated for 5 min at 70°C and then for 1 h at 37°C. The reaction was stopped by heating at 95°C for 5 min.

The cDNA was used to perform SYBR-PCR based on SYBR-Green Fluorescence (FastStart Universal SYBR Green Master, Roche Diagnostics). Eight differentially expressed genes of interest (ATP-binding cassette, subfamily C [*abcc4*], cryptochrome 5 [*cry5*], N-myc downstream–regulated gene 1, like [*ndrg1l*], opsin 1 [cone pigments], medium wave–sensitive, 2 [*opn1mw2*], 3-phosphoinositide-dependent protein kinase-1 [*pdpk1*], period homolog 1 [*per1*], similar to son of sevenless homolog 2 [*sos*], and xeroderma pigmentosum, complementation group C [*xpc*]) were selected for confirmation of microarray results using qRT-PCR. Gene-specific primers were designed based on published zebrafish sequences (Table 1).

The following PCR reaction profile was used: one cycle at 95°C for 10 min followed by 40 cycles at 95°C for 15 s and 59°C for 60 s followed by a melting curve analysis after run.

The delta threshold cycle (CT) value was derived by subtracting the CT value for the housekeeping gene ribosomal protein L13 α (*RpL13α*), which served as an internal control, from the CT value of the target gene, respectively. All reactions were run in duplicate using the Biorad CFX96 RealTime PCR Detection System (Biorad, Reinach, Switzerland). The messenger RNA expression level of the different genes was expressed as fold increase according to the formula:

$$2^{\Delta CT(\text{untreated sample}) - \Delta CT(\text{treated sample})}$$

Measurement of Locomotor Activity

Multispecies Freshwater Biomonitor. Effects of PKC412 on locomotor activity were measured in zebrafish eleuthero-embryos. Their locomotor activity was observed using a flow-through test chamber with quadrupole impedance conversion as measuring device, connected to a measuring unit and personal computer with data analysis software (Gerhardt *et al.*, 1994). Measurement chambers, made of an acryl glass cylinder sealable on both ends, with a size of 4 cm in length and a diameter of 2 cm allowed free movement of the eleuthero-embryos during measurement.

For locomotor activity measurements, embryos in the blastula stage were exposed to 2.1 and 31 µg/l PKC412, respectively, for 6 dpf as described above. Locomotor activities of hatched eleuthero-embryos were assessed 6 dpf for 20 animals per PKC412 dose and the appropriate controls, respectively, as described above. Following an acclimation phase of 10 min, measurements

were started and behavior was monitored with a recording duration lasting 4 min for a period of 2 h with intervals of 10 min each. For locomotor activity measurements, means of locomotor activities (percent time spent on locomotion) for each individual were calculated for 2-h time period.

Angiogenesis

Double-transgenic zebrafish embryos (Tg(fli1a:EGFP)y1;Tg(gata1:dsRed) sd2) (Lawson and Weinstein, 2002; Traver *et al*., 2003) were exposed to 2 and 40 μg/l PKC412 and held in water and DMSO control water (50 embryos each) for 6dpf as described above. Embryos were monitored for morphological defects using a fluorescent binocular at 24 hours postfertilization (hpf), 48 hpf, and 6dpf. Formation of blood vessels was observed with transgenic expression of enhanced green fluorescent protein in endothelial cells and red fluorescent protein from *Discosoma* sp. expression in blood cells. Transgenic fish were kept heterozygotic; therefore, only half of the progeny is double transgenic and these were analyzed in detail. Representative embryos taken from treated and control groups were imaged using a Leica TCS SP5 Confocal Microscopy System.

Apoptosis Assay

Apoptotic cells of eleuthero-embryos were determined by the TUNEL assay. Eleuthero-embryos were exposed 6 dpf as described above. Embryos exposed to 1% H_2O_2 served as a positive control. After 6 dpf, the eleuthero-embryos were fixed in 4% Roti-Histofix at 4°C for 24 h. Thereafter, the embryos were rehydrated through a series of methanol (100, 90, 70, and 50%). The TUNEL assay (Roche "*In situ* Cell Death Detection Kit, TMR red") was performed as described in the manufacturer's manual. In brief, single eleuthero-embryos ($n = 3$ per replicate) were permeabilized in PBS containing 0.1% Triton X-100 for 8 min. Thereafter, they were washed twice with PBS and then labeled for 60 min at 37°C. The embryos were then embedded in agarose and analyzed under the fluorescent microscope at excitation and emission wavelength of 360–370 and 420 nm, respectively.

Alkaline Comet Assay

This assay allows detecting DNA breakages induced by genotoxic agents. The comet assay was performed as described (Duong *et al*., 2010). Briefly, embryos were exposed to PKC412 as described above for 6 dpf. As a positive control, embryos were exposed to 1% H_2O_2 for 10 min prior to anestization. A pool of eight eleuthero-embryos per replicate ($n = 4$) was macerated in 1 ml PBS containing 20mM EDTA for 5 min. The supernatant was removed, and the embryos were shred in 500 μl PBS containing 20mM EDTA for 10 min. The remaining tissue was sedimented for 2 min, and the supernatant was embedded in agarose on a microscope slide. Cells were then lysed at 4°C for 1 h with lysis buffer (2.5M NaCl, 0.1M EDTA, 10mM Tris-HCl, pH 10, 1% Triton X-100) and electrophoresed for 5 min at 25 V. Damaged DNA fragments migrate faster in the electric field than intact DNA, which can be visualized after staining with DAPI. Cells (24 cells per replicate) were observed under the fluorescence microscope, and the length of comets, percent DNA in tail, tail moment, and olive tail moment were calculated using CometScore 1.5 (TriTek, Sumerduck, VA).

ROS Measurements

In this assay, the nonfluorescent probe DCFH-DA is oxidized into the highly fluorescent 2,7-dichlorofluorescein in the presence of ROS. ROS measurements were conducted according to Deng *et al*. (2009). In brief, eight pre-exposed eleuthero-embryos (pre-exposure for 6 dpf as described for the microarray experiment) were washed with cold PBS and then homogenized in cold lysis buffer containing 0.32mM sucrose, 20mM HEPES, 1mM $MgCl_2$, and 0.5mM AEBSF, pH 7.4. As a positive control, eight eleuthero-embryos were exposed for 10 min to water containing 1% H_2O_2. Thereafter, the homogenate was centrifuged at 15,000 × g at 4°C for 20 min, and the supernatant was discharged. The pellet was then resuspended in PBS, and 20 μl were added to a 96-well plate and incubated for 5 min at room temperature. Thereafter, 100 μl of PBS and 8.3 μl of DCFH-DA (stock solution in DMSO, 10 mg/ml) were added to each well. The plate was incubated at 37°C for 30 min, and fluorescence measurements were made with excitation at 485 nm and emission at 530 nm, respectively.

Data Analysis and Statistics

Raw microarray data were analyzed using the GeneSpring GX 10 software (Agilent Technologies). In a first step, the Agilent FE software output was filtered on the basis of feature saturation, nonuniformity, pixel population consistency, and signal strength relative to background level (Agilent FE Manual). Only positively marked entities were accepted for further evaluation. All data were quantile normalized. In a second step, several quality control steps (e.g., correlation plots and correlation coefficients, quality metric plots, and principal components analysis) using the quality control tool of GeneSpring were performed to ensure that the data were of good quality.

Differentially expressed genes from the microarray were determined using a Benjamini-Hochberg multiple correction ANOVA test ($p < 0.05$) followed by a Tukey honestly significant difference technique *post hoc* test. The genes were considered differentially expressed when $p < 0.05$ and the fold change (FC) ≥ 2. To determine gene ontology (GO) categories of differentially expressed genes, the GO analysis tool in GeneGo, San Diego, CA, was used. Only those categories where $p < 0.05$ were considered differentially altered. MetaCore (GeneGo) was used to identify and visualize the involvement of the differentially expressed genes in specific pathways (false discovery rate [FDR] < 0.05). The microarray data used in this analysis have been submitted to the National Center for Biotechnology Information Gene Expression Omnibus database under accession number GSE23156 (http://www.ncbi.nlm.nih.gov/geo/query/acc.cgi?token=fnotryskkqyaoba&acc=GSE23156).

Data from microarray analysis, qRT-PCR, locomotor activity, comet assay, and ROS assay were illustrated graphically with GraphPad Prism 5 (GraphPad Software, San Diego, CA). Data distribution for normality was assessed with the Kolmogorov-Smirnov test and the variance homogeneity with the Bartlett test. Differences between treatments were assessed by ANOVA followed by a Tukey test (Bartelett test $p < 0.05$) to compare treatment means with respective controls. If the data were not normally distributed, differences between treatments were assessed by the Kruskal-Wallis test followed by Dunn's multiple comparison test. Results are given as mean ± SEM. Differences were considered significant at $p \leq 0.05$.

RESULTS

PKC412 Concentrations and Embryo Survival

PKC412 concentrations in the exposure water were measured at 0 and 24 h in order to determine the actual exposure concentrations. The PKC412 concentrations measured independently in the different experiments are given in Table 2. In the microarray experiment, actual concentrations were lower than nominal, and they decreased during exposure. Geometric mean concentrations ($n = 3$) were 1.3 and 21 μg/l. Also in the behavioral experiment using the Multispecies Freshwater Biomonitor (MFB), the PKC412 concentration decreased during the 24-h exposure and the mean measured concentration was 2.1 and 31 μg/l. In the experiments where the comet assay, TUNEL assay, and ROS assay were performed, the initial concentrations were close to nominal and decreased again during the 24-h exposure. The mean measured concentrations were 1.6 and 31 μg/l. No significant mortality was observed in any of the different experiments and treatment groups.

Alteration of Gene Expression

Gene expression profiles derived from microarray results of control and PKC412-exposed embryos ($n = 4$) are based on 80

TABLE 2
Nominal and Measured Concentrations of PKC412 in Exposure Waters after 6 dpf of Exposure for the Microarray, Multispecies Freshwater Biomonitor Experiment and Comet Assay

	Exposure waters				
	Measured concentration (µg/l)				
Nominal concentration	0 h	% Nominal	24 h	% Nominal	Geometric mean
Microarray					
2 µg/l	1.50 ± 0.1	75.2	1.06 ± 0.2	52.9	1.3
40 µg/l	25.12 ± 1.6	62.8	17.20 ± 3.1	43.0	21
Multispecies Freshwater Biomonitor					
2 µg/l	2.36 ± 0.1	117.8	1.90 ± 0.2	95.1	2.1
40 µg/l	37.45 ± 1.7	93.6	25.10 ± 1.7	62.7	31
TUNEL assay, comet assay, and ROS assay					
2 µg/l	2.19 ± 0.2	109.5	1.23 ± 0.1	61.7	1.6
40 µg/l	38.60 ± 6.4	96.5	24.93 ± 5.2	62.3	31

TABLE 3
FCs of Selected Genes Differentially Regulated in Zebrafish Eleuthero-Embryos Determined by Microarray and qRT-PCR after Exposure to 1.3 and 21 µg/l PKC412. Values Are Expressed as Average FC. Asterisks Show Statistically Significant Difference to Control ($p < 0.05$)

	FC (log_2)			
	1.3 µg/l PKC412		21 µg/l PKC412	
Gene name	Array	qPCR	Array	qPCR
abcc4	−2.00*	−1.21*	−2.98*	−1.03*
cry5	−2.68*	−2.35*	−2.86*	−2.12*
ndrg1l	4.00*	1.99*	4.10*	2.41*
opn1mw2	2.60*	0.45*	2.36*	1.00*
pdpk1	2.60*	0.88*	1.71*	1.05*
per1	−9.80*	−3.58*	−6.41*	−3.16*
sos	0.85*	−0.27	2.03*	0.62
xpc	−2.90*	−1.40*	−2.20*	−0.55

pooled individuals. As listed in Supplementary table S1, 259 and 511 genes were differentially expressed in zebrafish eleuthero-embryos ($log_2 \geq 2$, $p < 0.05$) after exposure to 1.3 and 21 µg/l PKC412, respectively. At 1.3 µg/l PKC412, 112 (43%) genes were downregulated and 147 (57%) upregulated. Of the 511 genes differentially expressed at 21 µg/l PKC412, 130 (25%) genes were downregulated and 381 (75%) were upregulated. Only 101 of the significantly altered genes were regulated at both concentrations; however, all of them were regulated in the same direction. At both concentrations, most functional groups of genes (FC, log_2 at least twofold, $p \leq 0.05$) were similar. GO analysis was performed to identify functional groups of genes. GO defines terms representing gene product properties and covers three domains, namely, cellular components, molecular functions, and biological processes. At both concentrations, functionally identified genes fell into more than 1500 different categories. In Supplementary table S2, the top 100 GO processes are listed. GO categories including all kind of different detections or responses to stimuli are of particular importance, e.g., detection of light stimulus, detection of abiotic stimulus, detection/response to external stimulus, visual perception, etc. (Supplementary table S2).

In addition to the GO analysis, we performed a pathway analysis with MetaCore. The different treatments had 28 maps (1.3 µg/l PKC412: 29 maps; 21 µg/l PKC412: 34 maps) with their corresponding pathways in common (Supplementary table S3). These maps include pathways for lipid biosynthesis and regulation, cholesterol and bile acid homeostasis, angiogenesis, vitamin and cofactor metabolism and its regulation, mitogenic signaling, and apoptosis. For validation of these results, additional experiments were performed focusing on five significantly altered maps (Table 3). Effects on angiogenesis were analyzed by performing an additional experiment with transgenic zebrafish. In addition, effects on apoptosis were analyzed by performing a TUNEL assay, DNA damage was assessed by a comet assay, and oxidative stress response by a ROS assay.

In order to confirm the microarray results, qRT-PCR was performed for eight selected genes (Table 3, Fig. 1). These genes belong to different pathways and were selected on their importance in different pathways: *abcc4*, *cry5*, *ndrg1l*, *opn1mw2*, *pdpk1* 1, *per1*, *sos*, and *xpc*. A downregulation occurred for *abcc4*, *cry5*, *per1*, and *xpc*, whereas an upregulation was found for *ndrg1l*, *opn1mw2*, *pdpk*, and *sos* (Fig. 1, Table 3). In all cases, except *sos*, the same tendency for up- or downregulation occurred for the microarray and for qRT-PCR analysis.

Effects on the Circadian Rhythm and Locomotor Activity

As shown in Supplementary table S1, PKC412 altered the expression of genes regulating circadian rhythm, e.g., *cry1-5* (1.3 µg/l PKC412: −2.08, 3.9, −4.4, 2.3, −2.7 FC log_2, respectively; 21 µg/l PKC: −1.54, 2.7, −3, 1.8, −2.9 FC log_2, respectively), *per1,2,4* (1.3 µg/l PKC412: −9.8, −2.04, −4.5 FC log_2, respectively; 21 µg/l PKC: −6.4, −3.08, −3.17 FC log_2, respectively), *arntl* (1.3 µg/l PKC412: 2.5 FC log_2; 21 µg/l PKC: 3.12 FC log_2), *clock* (1.3 µg/l PKC412: 2.9 FC log_2; 21 µg/l PKC: 2.7 FC log_2), etc. In mammals, the circadian rhythm controls a diversity of behavioral and physiological rhythmic processes such as regulation of sleep wakefulness, secretion of hormones, and locomotor activity (Hastings, 1997). In zebrafish, diazepam alters the same set of genes and influences the swimming behavior (Oggier *et al.*, 2010). Therefore, an additional set of experiments was performed to evaluate whether changes found in the gene expression pattern of circadian genes

TABLE 4
Four Maps and Pathways to Which Additional Experiments Were Performed Represented in MetaCore (FDR < 0.05)

Map	Pathway	*p* Value
Vascular development (angiogenesis)	Transcription_Role of Akt in hypoxia-induced HIF1 activation	3.414×10^{-2}
	Transcription_Receptor-mediated HIF regulation	
	Development_FGFR signaling pathway	
Apoptosis	Transcription_P53 signaling pathway	5.423×10^{-2}
	Development_Flt3 signaling	
	Apoptosis and survival_Role of CDK5 in neuronal death and survival	
	Apoptosis and survival_BAD phosphorylation	
	Apoptosis and survival_Antiapoptotic action of gastrin	
	Apoptosis and survival_HTR1A signaling	
DNA damage response	Transcription_P53 signaling pathway	1.146×10^{-1}
	DNA damage_Role of Brca1 and Brca2 in DNA repair	
	DNA damage_Brca1 as a transcription regulator	
	DNA damage_Nucleotide excision repair	
	Apoptosis and survival_BAD phosphorylation	
Oxidative stress regulation	Development_Dopamine D2 receptor transactivation of EGFR	4.140×10^{-1}

Note. EGFR: epidermal growth factor receptor.

in eleuthero-embryos were paralleled by changes in the locomotor activity. The behavioral experiments revealed that exposure of the embryos to PKC412 did not significantly affect their locomotor activity (Supplementary fig. S1).

Effects on Angiogenesis

Angiogenesis is an important process during cancerogenesis, which is affected by PKC412 in humans (Fabbro *et al*., 2000). We hypothesized that similar effects occur in zebrafish embryos during development. Important genes in angiogenesis are the vascular endothelial growth factor (*vegf*), which is downregulated by PKC412 in humans (Fabbro *et al*., 2000), and angiopoietin (*ang*). In our study, we did not find a significant alteration in *vegf* transcript levels in zebrafish eleuthero-embryo (data not shown). However, there is a significant upregulation of *ang2* (3.6 FC $\log_2$) in the higher PKC412 concentration of 31 μg/l (Supplementary table S1). *Ang2* is an antagonist of *ang1* and disrupts blood vessel formation when overexpressed (Maisonpierre *et al*., 1997). In addition to alterations in gene expression, we also found a significant alteration of pathways involved in vascular development (Table 4).

In order to link these findings with physiological changes in blood vessel development, we exposed (Tg(fli1a:EGFP)y1;Tg(gata1:dsRed)sd2) double-transgenic zebrafish embryos to 2 and 40 μg/l PKC412. Although focusing mostly on the trunk vasculature, we did not observe any abnormalities in cardiovascular development compared with control embryos. At 24 hpf, the dorsal aorta and the posterior cardinal vein developed normally and normal sprouting of the intersegmental vessels was observed. At 6 dpf, all the main vessels looked virtually identical in treated and control embryos (Fig. 2). Dorsal aorta, posterior cardinal vein, and intersegmental vessels were normally developed, and normal heart beat and blood flow was observed.

Twenty-five double-transgenic embryos from each treatment were analyzed in detail. We also looked at general morphology of the embryos. Single embryos from treated and control groups showed mild developmental abnormalities, which can occasionally be observed in nontreated fish, especially in transgenic lines. Five of 25 embryos treated with 40 μg/l PKC412 had a slightly misshaped trunk with the tail bend dorsally. However, the vasculature of these embryos was normal (Fig. 2). More analyses on wild-type embryos would be needed to find out whether this misshaping is because of the drug treatment.

Therefore, PKC412 did not negatively interfere up to 6 days with the vascular development of zebrafish embryos at both concentrations. However, the vascular network at this stage is already very complicated and subtle differences might have been gone unnoticed.

Effects on Apoptosis in Olfactory Placodes

PKC inhibitors can induce apoptosis in humans (Tenzer *et al*., 2001). Thereby, the phosphatidylinositol 3′-kinase (PI3K3)/Akt pathway is of high importance as the cytotoxic effect of PKC412 is mediated by this pathway. In the apoptosis pathway, the phosphoinositide-dependent kinase (PDK) 1 (also called PDPK1) leads to phosphorylation of v-akt murine thymoma viral oncogene homolog Akt and therefore to its activation. Constitutively active Akt results in an enhanced protection against apoptotic cellular insults. In contrast to findings in humans, we found an upregulation of *pdpk* (Supplementary table S1, 2.6 FC $\log_2$) in the lower PKC412 concentration.

In addition, we found a downregulation of transcripts of *xpc*, a gene that is important for DNA damage recognition. Additionally, apoptotic pathways are of significance (Table 4). Based on these findings, we conducted a TUNEL assay to search for regions and tissue in the eleuthero-embryo where apoptosis is induced by PKC412. Supplementary figure S2 illustrates that apoptosis mostly occurred in the head region. The olfactory placode, which is important for the perception of odorants, is mainly affected. This finding is in parallel to the observed upregulation of gene transcripts of some odorant receptors *or102-3* (2.8 FC $\log_2$) and *or11-10* (2.2 FC $\log_2$) found by microarray analysis for the highest PKC412 concentration (Supplementary table S1), suggesting a repair of these affected cells.

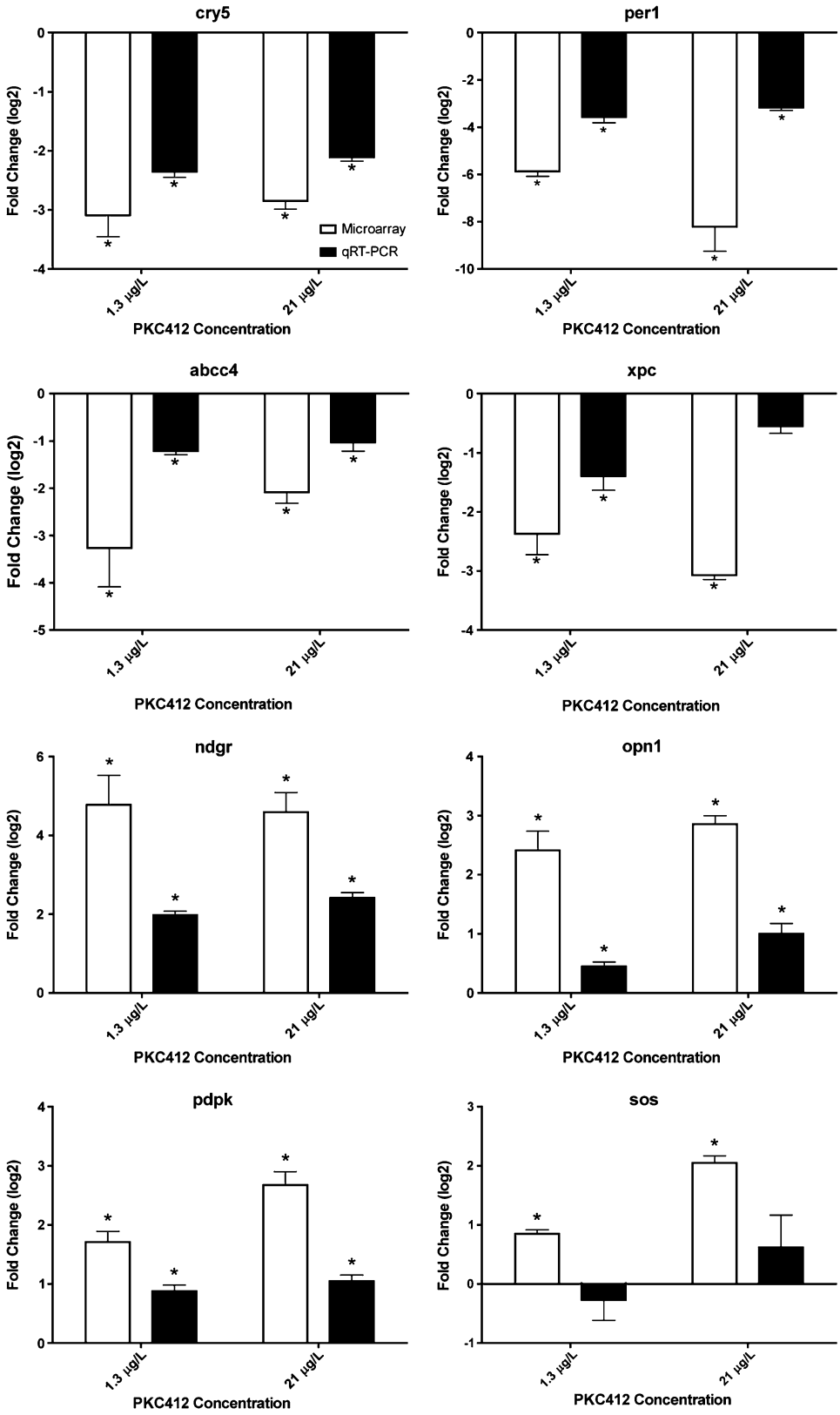

FIG. 1 Comparison of gene expression in zebrafish larvae determined by microarray ($n = 4$ replicates, 80 eleuthero-embryos pooled, white bars) and qRT-PCR ($n = 6$, 80 eleuthero-embryos, black bars) after exposure to 1.3 and 21 µg/l PKC412, respectively. Values are expressed as average FC ($\log_2$) with SE compared with control animals as indicated for selected genes. Asterisks (*) indicate statistically significant difference to control ($p < 0.05$).

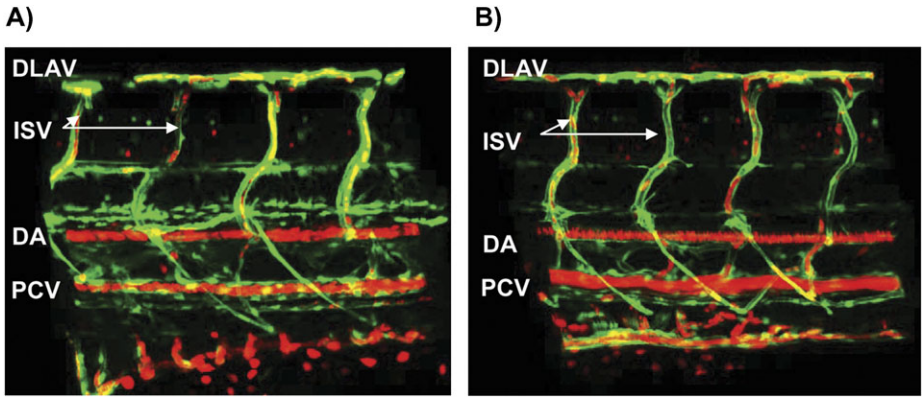

FIG. 2 Vascular development is not affected by PKC412 treatment. The vascular system was visualized in a double-transgenic zebrafish eleuthero-embryo (TG:fli1a:EGFPy1; gata1:DsRedsd2) on a Leica TCS SP5 Confocal Microscope. Endothelial cells are labeled in green and erythrocytes are labeled in red. (A) DMSO solvent control and (B) 40 μg/l PKC412. The pictures are maximal intensity projections of confocal z-stacks. DA, dorsal aorta; PCV, posterior cardinal vein; ISV, intersomitic vessel; DLAV, dorsal longitudinal anastomotic vessel. No major defects were detected in treated PKC412 embryos.

Effects on DNA Damage

PKC412 led to significant downregulation of *xpc*. At 1.6 and 31 μg/l PKC412, we found a 2.9 and 2.2 FC $\log_2$, respectively, in *xpc* transcripts (Table 3, Fig. 1). Additionally, there was a downregulation of *apex* nuclease 1 (-2.7 FC $\log_2$) at 31 μg/l PKC412. As *xpc* is important in DNA damage recognition and APEX1 for DNA repair, we conducted a comet assay to evaluate whether this alteration occurs not only on the transcription but also on the physiological level. Further support for potential DNA damage induced by PKC412 comes from the fact that pathways involved in DNA damage response were significantly affected (Table 4). The comet assay demonstrates a dose-dependent increase in DNA damage in eleuthero-embryos exposed to PKC412 (Fig. 3). Significant DNA damage occurred in the embryos at 31 μg/l PKC412. At the lower concentration of 1.6 μg/l PKC412, a significant increase in tail length, but not in percent DNA in tail, tail moment, and olive tail moment, occurred (Fig. 3).

Effects on Formation of ROS

MetaCore pathway analysis indicated that there is an alteration in oxidative stress regulation. To evaluate whether this is related to increased formation of ROS by PKC412, we performed an additional experiment to determine formation of ROS. The results show that the ROS levels remained unchanged at both PKC412 concentrations as compared with the control (Supplementary fig. S3), and thus PKC412 is not inducing ROS.

DISCUSSION

This is the first study investigating the effects of PKC412 on gene expression on nontarget organisms in aquatic systems. We show effects of PKC412 at low concentrations in zebrafish eleuthero-embryos. Thereby, we demonstrate that this human pharmaceutical exhibits its effects in aquatic organisms by similar molecular modes of action as in humans because of target conservation in vertebrates (Christen *et al.*, 2010 Gunnarsson *et al.*, 2008). We also tested the hypothesis that alteration in gene expression propagates into physiological effects.

PKC412 was designed as tyrosine kinase inhibitor with a broad inhibition spectrum of the human kinome. It was shown that at high-affinity interactions (Kd < 100nM), this compound was not highly selective for kinases (Karaman *et al.*, 2008). Consequently, it is not surprising that PKC412 alters more than 500 genes in zebrafish eleuthero-embryos at a concentration of 21 μg/l. Furthermore, the broad spectrum of kinases inhibited by the nonselective PKC412 makes the interpretation of the results challenging because of the involvement of many cellular pathways.

In humans, PKC412 inhibits FLT3, PDGF receptors, VEGF, and c-kit by preventing the tyrosine autophosphorylation (Fabbro *et al.*, 2000). In addition, this compound inhibits P-glycoprotein–mediated multidrug resistance in tumor cells. When comparing our results with human effects and gene expression changes obtained in MV4-11 cells (human lymphoblast cells) after treatment with 570 μg/l PKC412 (Stolzel *et al.*, 2010), some similarities show up. In zebrafish eleuthero-embryos, there were also alterations of solute carriers as in human cells (Stolzel *et al.*, 2010), albeit a solute carrier of family 2 was significantly downregulated in the lower concentration only. In addition, we similarly found a significant downregulation of the ABC transporter *abcc4*, which is important for the efflux of anticancer drugs. However, there was no alteration of *flt3*, *pdgfr*, *vegf*, and *c-kit* at the transcript level in zebrafish embryos. Binding of PKC412 leads to inhibition of these kinases; therefore, we hypothesize that PKC412 does not interfere with gene expression but protein function. One important identified GO category is visual

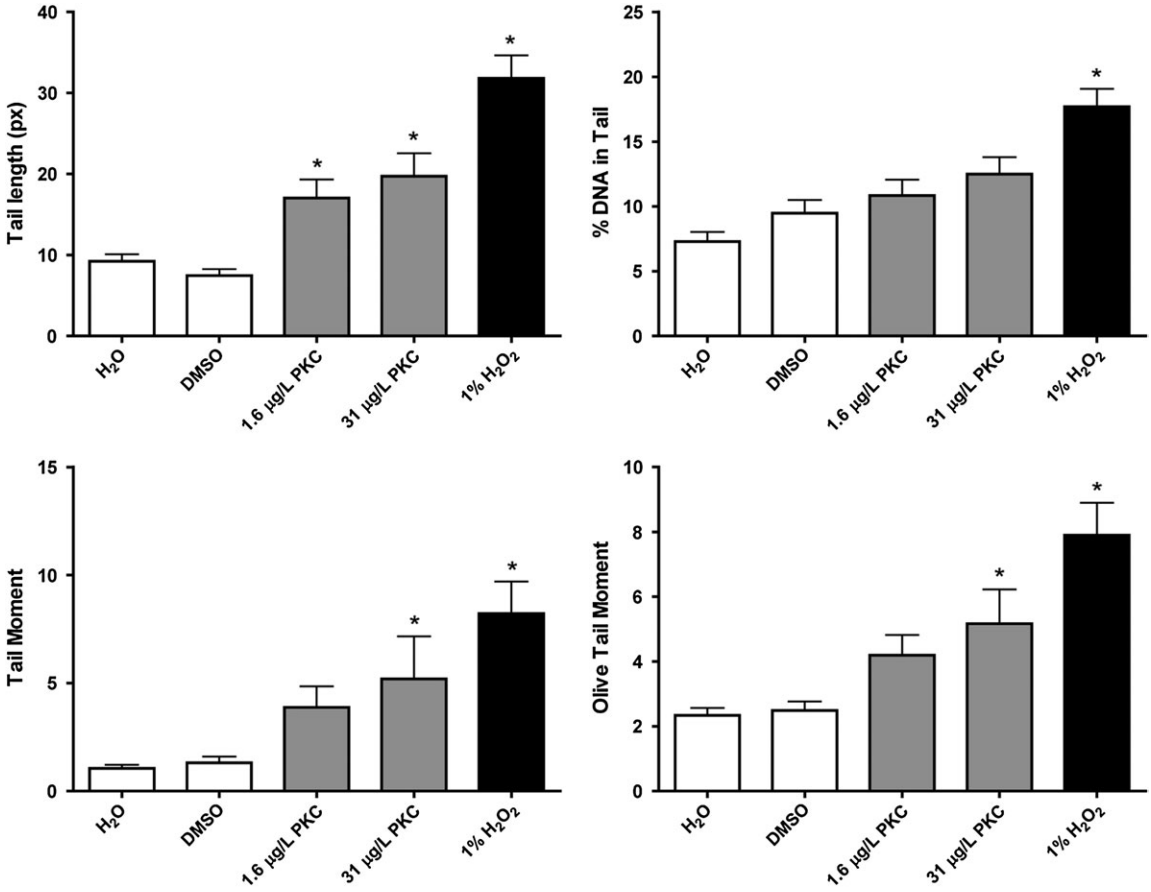

FIG. 3 Comet assay in zebrafish eleuthero-embryos exposed to 1.6 and 31 µg/l PKC412. (A) Tail length, (B) percent DNA in Tail, (C) Tail Moment, and (D) Olive Tail Moment were calculated using CometScore. Four slides per dosage were examined, and 24 cells per slide were scored. The values are presented as the mean ± SEM. Asterisks (*) indicate values that are significantly different from the control (Kruskall-Wallis test followed by *post hoc* Dunn's multiple comparison test; $p < 0.05$).

perception. Expression of genes encoding proteins involved in vision such as crystallins and opsins were significantly altered by PKC412. Crystallins are important for the protection against lens opacity (Clark, 2004), and opsins are important for dim-/daylight vision and color vision (Takechi and Kawamura, 2005). These findings in zebrafish are similar to results obtained in mice and humans after treatment with PKC412. There are several VEGF and PDGF receptors in the retina. The inhibition of these receptors can lead to decreased epiretinal membrane formation in mice (Saishin *et al*., 2003) and reduction in macular edema in humans (Campochiaro, 2004). Therefore, upregulation of crystallins and opsins may be a response to the inhibition of VEGF and PDGF receptors.

In addition to visual perception, we also found that responses to light and external/internal stimuli are important targets of PKC412. As the circadian rhythm is dependent on stimuli, namely, Zeitgeber, there is a significant alteration of those genes at both PKC412 concentrations in zebrafish. It is known that in mice, several protein kinases C are expressed in the hypothalamic suprachiasmattic nuclei (SCN) (Van der Zee and Bult, 1995), the region which is important for circadian processes. Therefore, protein kinases C play an important role in the mammalian circadian rhythm, and inhibition of PKC can lead to phase advances (Jakubcakova *et al*., 2007; Schak and Harrington, 1999). As PKC is already expressed in the early zebrafish development (Patten *et al*., 2007; Slatter *et al*., 2005), it could be affected in the SCN. Additionally, it was shown in the marine dinoflagellate *Lingulodinium polyedrum* that staurosporine (precursor of PKC412) leads to phase shifting and it increases the free running period of the circadian rhythm (Comolli and Hastings, 1999). At the behavioral level, altered expression of clock genes is correlated with changes in the locomotor activity (Jakubcakova *et al*., 2007). For this reason, we investigated the effects of PKC412 on the locomotor activity. However, PKC412 had no significant effect on the locomotor activity in our experimental setup. A reason could be that an observation over 2 h is too short to obtain significant effects. Also the time point when the measurements took place could have an influence. We performed our measurements at daylight, and effects would have probably been more pronounced at night.

In addition to exploring effects on different GO categories, we performed a pathway analysis in order to elucidate altered maps and pathways after PKC412 exposure. Out of the 28 maps, we chose four different maps with their corresponding pathways to perform additional experiments. It is known from humans that PKC412 can have effects on angiogenesis and apoptosis including DNA damage repair. However, there are no indications from mammalian studies that PKC412 exposure can lead to the formation of ROS.

The need for new blood vessels is important during embryogenesis, as well as in processes during cancerogenesis (Carmeliet and Jain, 2000). The formation of blood vessels and evaluation of blood flow can be observed in zebrafish eleuthero-embryos, rendering it an ideal model organism to study angiogenesis. As angiogenesis is affected by PKC412 in humans (Fabbro *et al*., 2000), we hypothesize that similar effects occur in zebrafish eleuthero-embryos. Thereby, angiopoietins play an important role (Kubota *et al*., 2005; Pham *et al*., 2001). In fact, we found a significant upregulation of *ang2*. It was shown that overexpression of *ang2* can lead to blood vessel disruption in the mouse embryo (Maisonpierre *et al*., 1997). There is also a simultaneous regulation of VEGF and angiopoietin. However, angiopoietins do not participate in the initial vascular phase of vascular development but rather play an important role in angiogenic outgrowth, vessel remodeling, and maturation (Dumont *et al*., 1994; Suri *et al*., 1996). Our results obtained after the exposure of double-transgenic zebrafish eleuthero-embryos support the findings that angiopoietins do not participate in the initial vascular phase. In addition, our findings are in agreement with those obtained after exposure of zebrafish eleuthero-embryos to 57 μg/l for 24 hpf (Chan *et al*., 2002). PKC412 did not generate measurable antiangiogenic effects during the exposure time. It may be possible that there are strain differences between zebrafish that account for our failure to detect vascular defects in transgenic fish. However, our results are in line with the microarray data in the sense that we did not find any alteration in *vegf* transcript levels. In addition, the defects in the vasculature might be too subtle to detect upon PKC412 treatment, so that they went unnoticed in our assays.

PKC inhibitors can induce apoptosis in humans (Tenzer *et al*., 2001). To protect mammals from apoptotic stress stimuli, the PI3K/Akt survival pathway is important. In this pathway, Akt needs to be phosphorylated by the PDK1, which was found to be downregulated in mice after treatment with staurosporine (Hill *et al*., 2001). In mice, PKC412 can mediate its cytotoxic effects partly via downregulation of this pathway. Additionally, PKC412 decreased the site-specific phosphorylation of Akt required for its activity (Tenzer *et al*., 2001). In contrast to these findings, we found an upregulation of the upstream *pdpk1* at the lower PKC412 concentration. This leads to the hypothesis that there is no downregulation of the Akt pathway but a protection against apoptosis. However, there is the indication that the failure in DNA damage recognition (downregulation of *xpc*) is more important, and therefore, apoptosis is induced in limited regions of the eleuthero-embryo. The TUNEL assay showed that apoptotic cells were located in the olfactory placodes (fig. S2). As there is also an upregulation of odorant receptors, which are mainly expressed in the olfactory placodes, we suggest that this is a reaction to the damage and associated to repairing the loss of cells. Yet, there is no evidence for this phenomenon in mammals.

DNA damage can be paralleled with apoptosis. To evaluate whether alterations in *xpc* and *apex* can be linked to DNA damage, we performed comet assays. There is a clear link between gene expression alteration and DNA damage at both PKC412 concentrations. Although there is not significantly more DNA in the tail, there is a significant increase in tail length indicating that DNA damage took place. Data from the comet assay demonstrate that gene expression changes in DNA damage recognition are paralleled with intracellular DNA damage. These data are in agreement with the results obtained in human lymphoblast cells after treatment with PKC412 (Seedhouse *et al*., 2006).

We also showed that physiological outcomes of maps of low significance, as the regulation of oxidative stress, do not correlate with the obtained gene expression. Nevertheless, several markers such as metallothionein (*mt*, 2.3-fold downregulated at 21 μg/l) and glutathione *S*-transferase M (*gstm*, 1.1- and 1.2-fold downregulated at 1.3 and 21 μg/l, respectively) were significantly altered. It is known that *mt* is upregulated by free radicals in rainbow trout cells (Kling and Olsson, 2000). Our findings on the alteration of *gst* are in contrast with those obtained in goldfish after treatment with gemfibrozil, which is supposed to downregulate the antioxidant defense system (Mimeault *et al*., 2006). However, the gene expression of other markers such as the superoxide dismutase (*sod*) or the catalase (*cat*) was not altered.

In our study, we demonstrate that the response of zebrafish eleuthero-embryo to different PKC412 concentrations is partly similar to the response in humans. Significant changes in gene expression occurred at low concentrations of 1.3 μg/l PKC412. This demonstrates that alterations in gene expression are more sensitive than mortality and physiological effects. Additionally, the gene expression profile points to the modes of action of PKC412 in zebrafish. Because of the very broad kinase inhibition spectrum of PKC412, a correlation to physiological alterations is difficult. In some cases, gene expression changes were not paralleled by physiological changes at low concentrations and sometimes even at high concentrations. This raises the question whether and when gene expression changes propagate to toxicological relevant measures such as reduction of the ability to find food, to reproduce, or to escape from predators.

In conclusion, the present study confirms that the toxicogenomic approach provides important data to identify and characterize molecular effects and to investigate potential modes of action of an antineoplastic agent. This allows for establishing

new biomarkers, not regularly assessed in routine ecotoxicological studies. PKC412-induced alterations of gene transcripts were partly paralleled by physiological effects at high, but not at low, PKC412 concentrations that may be of environmental relevance. Our study also shows that molecular studies should be paralleled with ecotoxicological investigations of known ecological relevance to interrelate sensitive changes in gene expression to physiological effects.

SUPPLEMENTARY DATA

Supplementary data are available online at http://toxsci.oxfordjournals.org/.

FUNDING

Novartis Pharma AG; Novartis International AG; F. Hoffmann-La Roche Ltd. to K.F.

ACKNOWLEDGMENTS

We thank Andreas Hartmann (Novartis Pharma AG) and Jürg O. Straub (F. Hoffmann-La Roche Ltd) for support and reading the manuscript; Jakob Pernthaler (University of Zürich) for continuous support; Andrea Patrignani, Sabina Wirth, and Hubert Rehrauer (Functional Genomics Center Zurich) for their technical and statistical support; Almut Gerhardt and Cornelia Kienle (Ecotoxicology Center, Dübendorf) for help with the MFB study; Tim Chico (University of Sheffield, UK) for double-transgenic zebrafish; Elín Ellertsdóttir (Biozentrum, University of Basel) for supervising the angiogenesis experiment; Armin Zenker, Jennifer Morger, Christian Kropf, and Verena Christen for technical assistance; and Roger Gruner (Harlan Laboratories Ltd) for providing zebrafish eggs. Birgit Hoeger is employed by Novartis Pharma AG, who owns the patent on PKC412. The authors declare that they have no conflicts of interest.

REFERENCES

Campochiaro, P. A. (2004). Reduction of diabetic macular edema by oral administration of the kinase inhibitor PKC412. *Invest. Ophthalmol. Vis. Sci.* **45,** 922–931.

Carmeliet, P., and Jain, R. K. (2000). Angiogenesis in cancer and other diseases. *Nature* **407,** 249–257.

Chabner, B. A., Ryan, D. P., Paz-Ares, L., Garcia-Carbonero, R., and Calabresi, P. (2006). Antineoplastic agents. In *Goodman and Gilman's—The Pharmalogical Basis of Therapeutics* (Hardman, J. G. and Limbird, L. E., Eds.), pp. 1396–1397. McGraw-Hill, New York.

Chan, J., Bayliss, P. E., Wood, J. M., and Roberts, T. M. (2002). Dissection of angiogenic signaling in zebrafish using a chemical genetic approach. *Cancer Cell* **1,** 257–267.

Christen, V., Hickmann, S., Rechenberg, B., and Fent, K. (2010). Highly active human pharmaceuticals in aquatic systems: A concept for their identification based on their mode of action. *Aquat. Toxicol.* **96,** 167–181.

Clark, J. I. (2004). Order and disorder in the transparent media of the eye. *Exp. Eye Res.* **78,** 427–432.

Comolli, J. C., and Hastings, J. W. (1999). Novel effects on the Gonyaulax circadian system produced by the protein kinase inhibitor staurosporine. *J. Biol. Rhythms* **14,** 11–19.

Deng, J., Yu, L., Liu, C., Yu, K., Shi, X., Yeung, L. W., Lam, P. K., Wu, R. S., and Zhou, B. (2009). Hexabromocyclododecane-induced developmental toxicity and apoptosis in zebrafish embryos. *Aquat. Toxicol.* **93,** 29–36.

Dumont, D. J., Gradwohl, G., Fong, G. H., Puri, M. C., Gertsenstein, M., Auerbach, A., and Breitman, M. L. (1994). Dominant-negative and targeted null mutations in the endothelial receptor tyrosine kinase, tek, reveal a critical role in vasculogenesis of the embryo. *Genes Dev.* **8,** 1897–1909.

Duong, F. H., Christen, V., Lin, S., and Heim, M. H. (2010). Hepatitis C virus-induced up-regulation of protein phosphatase 2A inhibits histone modification and DNA damage repair. *Hepatology* **51,** 741–751.

European Medicines Agency (EMEA). (2006). *Guideline on the Environmental Risk Assessment of Medicinal Products for Human Use*. EMEA, London.

Fabbro, D., Ruetz, S., Bodis, S., Pruschy, M., Csermak, K., Man, A., Campochiaro, P., Wood, J., O'Reilly, T., and Meyer, T. (2000). PKC412—a protein kinase inhibitor with a broad therapeutic potential. *Anticancer Drug Des.* **15,** 17–28.

Fent, K., Weston, A. A., and Caminada, D. (2006). Ecotoxicology of human pharmaceuticals. *Aquat. Toxicol.* **76,** 122–159.

Gerhardt, A., Clostermann, M., Fridlund, B., and Svensson, E. (1994). Monitoring of behavioral patterns of aquatic organisms with an impedance conversion technique. *Environ. Int.* **20,** 209–219.

Gunnarsson, L., Jauhiainen, A., Kristiansson, E., Nerman, O., and Larsson, D. G. (2008). Evolutionary conservation of human drug targets in organisms used for environmental risk assessments. *Environ. Sci. Technol.* **42,** 5807–5813.

Hastings, M. H. (1997). Central clocking. *Trends Neurosci.* **20,** 459–464.

Hill, M. M., Andjelkovic, M., Brazil, D. P., Ferrari, S., Fabbro, D., and Hemmings, B. A. (2001). Insulin-stimulated protein kinase B phosphorylation on Ser-473 is independent of its activity and occurs through a staurosporine-insensitive kinase. *J. Biol. Chem.* **276,** 25643–25646.

Jakubcakova, V., Oster, H., Tamanini, F., Cadenas, C., Leitges, M., van der Horst, G. T., and Eichele, G. (2007). Light entrainment of the mammalian circadian clock by a PRKCA-dependent posttranslational mechanism. *Neuron* **54,** 831–843.

Jones, O. A., Voulvoulis, N., and Lester, J. N. (2007). Ecotoxicity of pharmaceuticals. In *Analysis, Fate and Removal of Pharmaceuticals in the Water Cycle* (Petrovic, M., and Barcelo, D., Eds.), pp. 387–424. Oxford, Elsevier.

Karaman, M. W., Herrgard, S., Treiber, D. K., Gallant, P., Atteridge, C. E., Campbell, B. T., Chan, K. W., Ciceri, P., Davis, M. I., Edeen, P. T., *et al.* (2008). A quantitative analysis of kinase inhibitor selectivity. *Nat. Biotechnol.* **26,** 127–132.

Kimmel, C. B., Ballard, W. W., Kimmel, S. R., Ullmann, B., and Schilling, T. F. (1995). Stages of embryonic development of the zebrafish. *Dev. Dyn.* **203,** 253–310.

Kling, P. G., and Olsson, P.-E. (2000). Involvement of differential metallothionein expression in free radical sensitivity of RTG-2 and CHSE-214 cells. *Free Radic. Biol. Med.* **28,** 1628–1637.

Kubota, Y., Oike, Y., Satoh, S., Tabata, Y., Niikura, Y., Morisada, T., Akao, M., Urano, T., Ito, Y., Miyamoto, T., *et al.* (2005). Cooperative interaction of Angiopoietin-like proteins 1 and 2 in zebrafish vascular development. *Proc. Natl. Acad. Sci. U.S.A.* **102,** 13502–13507.

Lawson, N. D., and Weinstein, B. M. (2002). In vivo imaging of embryonic vascular development using transgenic zebrafish. *Dev. Biol.* **248,** 307–318.

Maisonpierre, P. C., Suri, C., Jones, P. F., Bartunkova, S., Wiegand, S. J., Radziejewski, C., Compton, D., McClain, J., Aldrich, T. H., Papadopoulos, N., *et al.* (1997). Angiopoietin-2, a natural antagonist for Tie2 that disrupts *in vivo* angiogenesis. *Science* **277,** 55–60.

Mimeault, C., Trudeau, V. L., and Moon, T. W. (2006). Waterborne gemfibrozil challenges the hepatic antioxidant defense system and down-regulates peroxisome proliferator-activated receptor beta (PPARβ) mRNA levels in male goldfish (*Carassius auratus*). *Toxicology* **228,** 140–150.

Monteiro, S. C., and Boxall, A. B. (2010). Occurrence and fate of human pharmaceuticals in the environment. *Rev. Environ. Contam. Toxicol.* **202,** 53–154.

Oggier, D. M., Weisbrod, C., Stoller, A., Zenker, A., and Fent, K. (2010). Effects of diazepam on gene expression and link to physiological effects in different life stages in zebrafish. *Danio rerio*. *Environ. Sci. Technol.* **44,** 7685–7691.

Patten, S. A., Sihra, R. K., Dhami, K. S., Coutts, C. A., and Ali, D. W. (2007). Differential expression of PKC isoforms in developing zebrafish. *Int. J. Dev. Neurosci.* **25,** 155–164.

Pham, V. N., Roman, B. L., and Weinstein, B. M. (2001). Isolation and expression analysis of three zebrafish angiopoietin genes. *Dev. Dyn.* **221,** 470–474.

Robbens, J., van der Ven, K., Maras, M., Blust, R., and De Coen, W. (2007). Ecotoxicological risk assessment using DNA chips and cellular reporters. *Trends Biotechnol.* **25,** 460–466.

Runnalls, T. J., Hala, D. N., and Sumpter, J. P. (2007). Preliminary studies into the effects of the human pharmaceutical clofibric acid on sperm parameters in adult fathead minnow. *Aquat. Toxicol.* **84,** 111–118.

Saishin, Y., Takahashi, K., Seo, M. S., Melia, M., and Campochiaro, P. A. (2003). The kinase inhibitor PKC412 suppresses epiretinal membrane formation and retinal detachment in mice with proliferative retinopathies. *Invest. Ophthalmol. Vis. Sci.* **44,** 3656–3662.

Schak, K. M., and Harrington, M. E. (1999). Protein kinase C inhibition and activation phase advances the hamster circadian clock. *Brain Res.* **840,** 158–161.

Seedhouse, C. H., Hunter, H. M., Lloyd-Lewis, B., Massip, A. M., Pallis, M., Carter, G. I., Grundy, M., Shang, S., and Russell, N. H. (2006). DNA repair contributes to the drug-resistant phenotype of primary acute myeloid leukaemia cells with FLT3 internal tandem duplications and is reversed by the FLT3 inhibitor PKC412. *Leukemia* **20,** 2130–2136.

Si, M. S., Reitz, B. A., and Borie, D. C. (2005). Effects of the kinase inhibitor CGP41251 (PKC 412) on lymphocyte activation and TNF-alpha production. *Int. Immunopharmacol.* **5,** 1141–1149.

Slatter, C. A. B., Kanji, H., Coutts, C. A., and Ali, D. W. (2005). Expression of PKC in the developing zebrafish, *Danio rerio*. *J. Neurobiol.* **62,** 425–438.

Stolzel, F., Steudel, C., Oelschlagel, U., Mohr, B., Koch, S., Ehninger, G., and Thiede, C. (2010). Mechanisms of resistance against PKC412 in resistant FLT3-ITD positive human acute myeloid leukemia cells. *Ann. Hematol.* **89,** 653–662.

Suri, C., Jones, P. F., Patan, S., Bartunkova, S., Maisonpierre, P. C., Davis, S., Sato, T. N., and Yancopoulos, G. D. (1996). Requisite role of angiopoietin-1, a ligand for the TIE2 receptor, during embryonic angiogenesis. *Cell* **87,** 1171–1180.

Takahashi, I., Saitoh, Y., Yoshida, M., Sano, H., Nakano, H., Morimoto, M., and Tamaoki, T. (1989). UCN-01 and UCN-02, new selective inhibitors of protein kinase C. II. Purification, physico-chemical properties, structural determination and biological activities. *J. Antibiot. (Tokyo)* **42,** 571–576.

Takechi, M., and Kawamura, S. (2005). Temporal and spatial changes in the expression pattern of multiple red and green subtype opsin genes during zebrafish development. *J. Exp. Biol.* **208,** 1337–1345.

Tenzer, A., Zingg, D., Rocha, S., Hemmings, B., Fabbro, D., Glanzmann, C., Schubiger, P. A., Bodis, S., and Pruschy, M. (2001). The phosphatidylinositide 3'-kinase/Akt survival pathway is a target for the anticancer and radiosensitizing agent PKC412, an inhibitor of protein kinase C. *Cancer Res.* **61,** 8203–8210.

Ternes, T. A. (1998). Occurrence of drugs in German sewage treatment plants and rivers. *Water Res.* **32,** 3245–3260.

Traver, D., Paw, B. H., Poss, K. D., Penberthy, W. T., Lin, S., and Zon, L. I. (2003). Transplantation and *in vivo* imaging of multilineage engraftment in zebrafish bloodless mutants. *Nat. Immunol.* **4,** 1238–1246.

Van der Zee, E. A., and Bult, A. (1995). Distribution of AVP and Ca2+-dependent PKC-isozymes in the suprachiasmatic nucleus of the mouse and rabbit. *Brain Res.* **701,** 99–107.